Non-Equatorial Uniform-Stress Space Elevators*

Blaise Gassend†

Abstract

Non-equatorial space elevators are interesting as they give more freedom for anchor location, avoid the highly occupied geosynchronous orbit and the areas of highest radiation in the Van Allen belts. We review the static equation for a uniform-stress tether, and use it to study the tapering of a uniform-stress tether in a general potential field. We then focus on a rotating coulomb potential and study the range of latitudes that are allowed for a uniform-stress space elevator. Finally, we look at a few practical issues that are raised by non-equatorial space elevators.

Introduction

A space elevator is a very long tether. One end is attached to an anchor station on the surface of a planet. The other end is attached to a counterweight located beyond the planet's synchronous altitude. Past that altitude centrifugal force due to the planet's rotation exceeds the gravitational force, so the counterweight is pulled away from the planet. Thus, the tether is kept in tension between anchor and counterweight. Payloads can be sent into space by climbing the tether, much more efficiently than with rockets.

The space elevator concept was first proposed in Russian [2, 3] by Artsutanov, and later introduced in English by Pearson [4]. Science fiction writers [5] made the idea popular. But materials with the necessary strength to weight ratio seemed unlikely. And the proposed elevators were much too heavy for foreseeable launch technologies. This changed with the arrival of carbon nanotubes, and the proposal by Edwards [1] of a space elevator concept that would only require a few tons of material to be lifted by conventional launch means.

To date, studies have considered that the space elevator would be anchored on the equator, as that is where the equilibrium of the tether is easiest to understand. Clarke [5] even considered that the elevator would have to be placed on the equator at a local minimum of the Earth's geopotential. In fact, there is no reason for such limitations, and non-equatorial space elevators can present a number of advantages:

- There is increased flexibility in the selection of the anchor location.
- The tether does not have to go through the heavily occupied (geo)synchronous orbit.
- The tether avoids the areas of most intense radiation of the Van Allen belts [6]. This is particularly important when considering the transportation of humans.
- The tether can avoid the Martian moons (in the case of a Martian elevator).

Figure 1 shows a diagram of a non-equatorial space elevator. Three forces hold it in equilibrium: gravity, centrifugal force, and the tension at the anchor. The major difference with equatorial elevators is that the elevator is located entirely on one side of the equatorial plane. Therefore, gravity tends to pull the elevator towards the equatorial plane. This tendency is countered by the force applied by the anchor, allowing the elevator to be in equilibrium.

In this paper we will be considering uniform-stress space-elevators. A uniform-stress tether is a tether in which the cross-section is varied (tapered) in order to keep the stress in the tether uniform. Space elevators are generally designed to have uniform stress as this maximizes the ratio of payload mass to elevator mass.

To understand off-equator space elevators, we will first review the static equations that any uniform-stress tether must satisfy, in Section 1. Then we will apply these equations to the relevant case of a rotating Coulomb potential in Section 2. In Section 3 we

†The author may be contacted at gassend@alum.mit.edu.

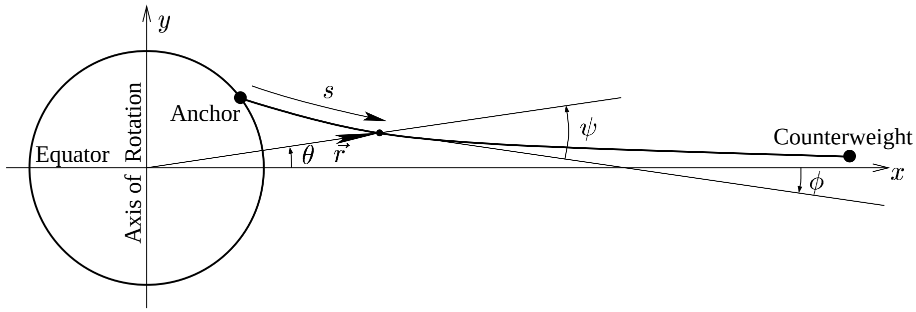

Figure 1: A non-equatorial space elevator, and some of the angles that are used to characterize it.

will study the problem of determining the maximum latitude a space elevator can start from. Finally, Section 4 covers a few practical concerns that are specific to non-equatorial space elevators.

All the notation that is used in this paper can be found in Table 1. Examples will often use values that are typical for Earth and the tethers considered by Edwards [1]. Table 2 summarizes these values.

1 Equations for a Static Uniform Stress Tether

First we introduce the equations for a static uniform-stress tether in a potential V.

$$\frac{\mathrm{d}\vec{r}}{\mathrm{d}s} = \frac{\vec{T}}{T} \tag{1}$$

$$\frac{\mathrm{d}\vec{T}}{\mathrm{d}s} = \rho\, A\, \vec{\nabla} V \tag{2}$$

$$T = \sigma_0\, A \tag{3}$$

In these equations s is a curvilinear coordinate along the tether, $\vec{T}$ is the tension that the top part of the tether applies to the bottom part, $\vec{r}$ is a position vector, A is the position dependent cross-sectional area of the tether, ρ is the density of the tether, and σ_0 is the stress in the tether. Equation (1) expresses that the tether cannot bear any shear load: the tension in the tether must be tangent to the cable. Equation (2) expresses Newton's second law: the change in tension along a small piece of tether must oppose the force due to the potential. Equation (3) expresses that the tether has a uniform stress. Because the tether is uniformly stressed, we need not consider elastic effects as they can be incorporated into σ_0 and ρ.

Equations (2) and (3) can be combined to eliminate the area of the cable.

$$\frac{\mathrm{d}\vec{T}}{\mathrm{d}s} = \frac{\rho T}{\sigma_0} \vec{\nabla} V \tag{4}$$

1.1 Taper Profile

First we shall look at the tangential part of the static equations. Integrating them will lead to a relation between the cable cross-section A and the local potential V.

First, we take the dot product of (4) with $\mathrm{d}\vec{r}$, divide by T, and use (1) to simplify.

$$\frac{\mathrm{d}T}{T} = \frac{\rho}{\sigma_0}\, \mathrm{d}\vec{r} \cdot \vec{\nabla} V \tag{5}$$

Integrating we get an expression for T and therefore for A.

$$\frac{T}{T_0} = \frac{A}{A_0} = e^{\frac{\rho}{\sigma_0} V} \tag{6}$$

This formula shows that the area of the tether at a given position is directly a function of the potential V at that position. If ΔV is the difference in potential energy between the base of the tether and the point where the potential energy reaches a maximum, then we can express the taper ratio of the tether as:

$$\frac{A_{max}}{A_0} = e^{\frac{\rho}{\sigma_0} \Delta V} \tag{7}$$

From this expression we can introduce a taper parameter $\frac{\rho}{\sigma_0} \Delta V$ that characterizes the difficulty of

Symbol	Description
s	Curvilinear coordinate along the tether.
$\vec{r}$	Position vector of a point on the tether.
r	Distance from the center of the planet.
$r_\perp$	Distance from the rotation axis of the planet.
r_s	Distance from the center of the planet to the synchronous altitude.
ρ	Density of tether material under stress.
σ_0	Target stress in tether.
A	Cross-sectional area of tether.
$\vec{T}$	Tension applied by the top part of the tether to the bottom part.
m	Mass of the counterweight.
V	Potential field the tether is placed in.
θ	Angle between the equatorial plane and the position vector $\vec{r}$.
ϕ	Angle between the equatorial plane and the tangent to the tether.
ψ	Angle between the tangent to the tether and the position vector $\vec{r}$
$\hat{e}_\phi$	Unit vector in the direction of increasing ϕ.
G	Gravitational constant.
M_p	Mass of the planet.
Ω	Angular velocity of planet rotation.
V_0	Characteristic specific energy of the rotating Coulomb potential field.
ΔV	Difference in potential between the base of the tether and the point where the potential is greatest.
$\vec{\tilde{g}}$	Combined gravitational and centrifugal field, in normalized form.
α	Tether shape factor.
P/M	Payload to tether mass ratio.
$(\vec{v})_\perp$	Part of some vector $\vec{v}$ that is normal to the tether.
$\tilde{d}$	Distance d in units of r_s.
$\breve{d}$	Distance d in units of αr_s.
x_0	The value of variable x at the anchor point (except V_0 and σ_0).

Table 1: Notation that is used in this paper.

building a uniform-stress structure across a potential difference ΔV. When it is much smaller than one, almost no tapering is necessary. When it is much larger than one the taper ratio becomes prohibitively large. This taper parameter is closely related to the ratio of Pearson's characteristic height [4] to the geosynchronous altitude.

Symbol	Typical Value
G	$6.67 \cdot 10^{-11}$ SI
M_p	$5.98 \cdot 10^{24}$ kg
Ω	$7.29 \cdot 10^{-5}$ rad/s
V_0	$9.46 \cdot 10^{6}$ J/kg
r_s	$42.2 \cdot 10^{6}$ m
r_0	$6.38 \cdot 10^{6}$ m
$\tilde{r}_0$	0.151
ρ	1300 kg/m^3
σ_0	$65 \cdot 10^{9}$ N/m^2
α	0.189

Table 2: Typical values for the Earth and Edwards' tether parameters [1]. When nothing is specified, these values are used for examples.

1.2 Tether Shape Equation

Projecting (4) onto a direction tangent to the tether allowed us to determine the taper profile. We now project perpendicularly to the tether direction and combine with (1) to determine the shape the tether adopts in the gravitational potential:

$$\frac{\mathrm{d}^2\vec{r}}{\mathrm{d}s^2} = \frac{\mathrm{d}\hat{T}}{\mathrm{d}s} = \frac{\rho}{\sigma_0}\left(\vec{\nabla}V\right)_\perp \tag{8}$$

where $\hat{T} = \vec{T}/T$ is a unit vector tangent to the tether, and $(\vec{\nabla}V)_\perp$ denotes the projection of $\vec{\nabla}V$ perpendicularly to $\hat{T}$.

Equation (8) determines the tether's curvature. The tether curves towards areas of higher potential, and the curvature is proportional to the component of the gravity field that is normal to the tether. This interpretation becomes more apparent in the case of a planar tether where we can identify the direction of the tether by an angle ϕ so that

$$\frac{\mathrm{d}\phi}{\mathrm{d}s} = \frac{\rho}{\sigma_0}\hat{e}_\phi \cdot \vec{\nabla}V \tag{9}$$

where $\hat{e}_\phi$ is a unit vector in the direction of increasing ϕ.

1.3 Boundary Conditions

To have a complete description of the static tether, we additionally need to consider boundary conditions. On one end, the tether is attached to the anchor point on the planet. The anchor simply needs to provide a force equal to the tension in the tether to keep the tether static. If the base of the tether isn't vertical then there will be a horizontal component to this force, so the tether will tend to pull the anchor sideways (see Section 4.2).

From equation (6) we know that the tension in the tether never goes to zero. Therefore, the free end of the cable must have a force applied to it to balance the tension in the cable. That force is provided by a counterweight of mass m which must satisfy:

$$\vec{T} = -m\vec{\nabla}V \tag{10}$$

Thus the counterweight must be located in such a way that the tether is tangent to the local gravity field.

2 The Rotating Coulomb Potential

So far we have considered a uniform stress tether in an arbitrary potential V. To make further progress, we will now consider the specific potential that applies in the case of the space elevator attached to a planet. Because we are considering the statics of the tether, we have to place ourselves in a reference frame that is rotating with the planet. Thus the potential we are interested in is a combination of the Coulomb potential of the planet's gravity and the centrifugal potential due to the planet's rotation around its axis:

$$V = -\frac{GM_p}{r} - \frac{1}{2}r_\perp^2\Omega^2 \tag{11}$$

In this equation G is the gravitational constant, M_p is the mass of the planet, Ω is the angular velocity of the planet's rotation, r is the distance to the center of the planet, and $r_\perp$ is the distance to the axis of rotation of the planet.

2.1 Planar Tether Profile

One of the first things we note about the potential is that it is invariant by reflection about planes that contain the planetary axis of rotation. This invariance must also apply to the resulting acceleration field. Thus, the forces caused by the potential will all be in a plane containing the axis of rotation and the point at which they are applied.

Therefore, if we consider a plane containing the axis of rotation of the planet and the counterweight, we find that the tension in the tether at the counterweight is in that plane. As we move down the tether, the forces acting on the tether are in that plane, so the tether remains in that plane all the way to the anchor.

We conclude that the shape of the space elevator will be planar, even in the non-equatorial case. This greatly simplifies the problem to be solved, as we can now work in two dimensions in a plane that is perpendicular to the equatorial plane.

2.2 Non-Dimensional Problem

Reducing a problem to non dimensional form is an excellent way of extracting the physically important parameters. We now apply this methodology to the space elevator.

First we note that the potential can be written in terms of the synchronous radius $r_s = (GM_p/\Omega^2)^{1/3}$ and the characteristic potential $V_0 = (GM_p\Omega)^{2/3}$ in the form:

$$V = -V_0\left(\frac{r_s}{r} + \frac{1}{2}\frac{r_\perp^2}{r_s^2}\right) \tag{12}$$

Thus, r_s, the distance from the center of the planet to the synchronous orbit, is the natural distance scale for this problem. We shall therefore rewrite (8) replacing all distances d by normalized distances $\tilde{d} = d/r_s$, and inserting the expression for V from (12):

$$\frac{\mathrm{d}^2\vec{\tilde{r}}}{\mathrm{d}\tilde{s}^2} = \frac{\rho V_0}{\sigma_0}\left(\frac{\vec{\tilde{r}}}{\tilde{r}^3} - \vec{\tilde{r}}_\perp\right)_\perp = -\alpha\left(\vec{\tilde{g}}\left(\vec{\tilde{r}}\right)\right)_\perp \tag{13}$$

This is the differential equation that determines the shape of the tether in a rotating Coulomb potential. This equation contains a single scalar parameter α which we shall call the shape parameter.

$$\alpha = \frac{\rho V_0}{\sigma_0} \tag{14}$$

The shape parameter is the ratio of the characteristic potential of the potential field to the strength

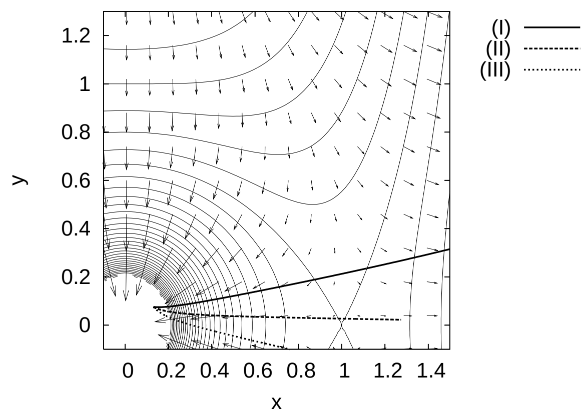

Figure 2: The normalized rotating Coulomb field $\vec{\tilde{g}}$. The equatorial plane is horizontal, and the North-South direction is vertical. Equipotential lines and field values are plotted along with three example tether solutions. The tether solutions are for $\alpha = 0.189$, $\tilde{r_0} = 0.151$, $\theta_0 = 30^\circ$ and inclinations ψ_0 of 35°, 55° and 75°.

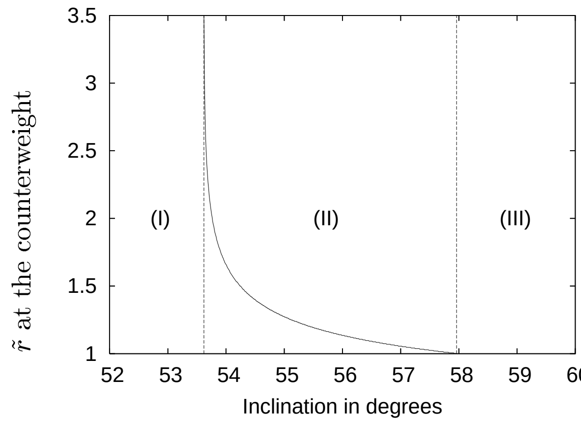

Figure 3: Normalized distance from the center of the Earth to the counterweight at latitude $\theta_0 = 30^\circ$.

to weight ratio of the tether material. It also naturally appears in (5), (6) and (7) when they are applied to the rotating Coulomb potential. The shape parameter determines how deep it is possible to go into the normalized potential well before the taper ratio becomes excessively high. Indeed, well below the synchronous altitude, $\Delta V \approx V_0 r_s/r$, so the taper parameter is approximately $\alpha/\tilde{r}$. Thus for $\alpha \ll \tilde{r}$, the taper ratio is close to 1, while for $\alpha \gg \tilde{r}$, the taper ratio is gigantic.

In the case of the Earth and the tether parameters from [1], $\alpha \approx 0.189$ and $\tilde{r} \approx 0.151$. Thus we are close to the limit of feasibility.

2.3 Solving the Shape Equation Qualitatively

To get an idea of the solutions of (13) that satisfy the boundary condition (10), it is useful to study Figure 2 which is a plot of the vector field $\vec{\tilde{g}}$. We shall assume without loss of generality that the anchor is in the upper right-hand quadrant ($x > 0$ and $y > 0$). More complete derivations can be found in [7].

To begin, we note that the North-South component of the field always points towards the equator. This has two consequences. First, because of (4) the y component of $\vec{T}$ satisfies:

$$y \frac{\mathrm{d}T_y}{\mathrm{d}s} > 0 \tag{15}$$

Second, because of (10), the tip of the tether at the counterweight has to be sloped towards the equatorial plane (i.e., $yT_y < 0$. Combining these two facts, we find that T_y is negative over the whole length of the tether. This implies via (1) that the distance from the tether to the equatorial plane must monotonically decrease as we move along the tether from the anchor point to the counterweight. If the tether ever crosses the equatorial plane, or starts heading away from the equatorial plane, the boundary condition will never be satisfied.

Below the synchronous altitude, $\vec{\tilde{g}}$ is pointing down and to the left. As we have seen, T is pointing down and to the right. Therefore because of (13) the tether only curves away from the equator (ϕ increases monotonically). We will use this result in Section 3.1.

Figure 2 shows how solutions of (13) depend on the inclination of the tether at the anchor. Case (II) satisfies the boundary condition at the counterweight, while (I) and (III) extend infinitely without the boundary condition ever being satisfied.

Indeed, if the inclination is too low as in case (I), then the tether curves away from the equatorial plane before suitable boundary conditions for a counterweight can be found. If the inclination is increased,

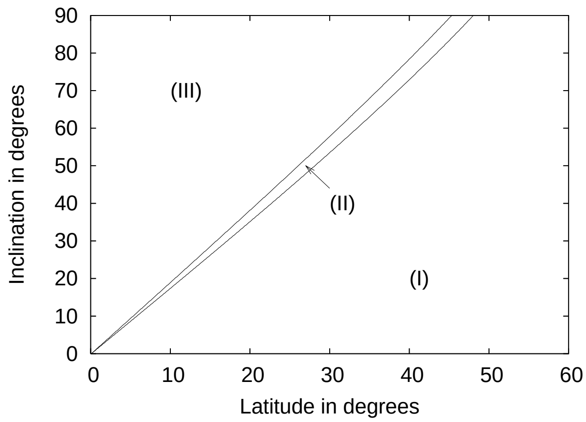

Figure 4: Possible inclinations for an Earth space elevator as a function of latitude ($\alpha = 0.189$).

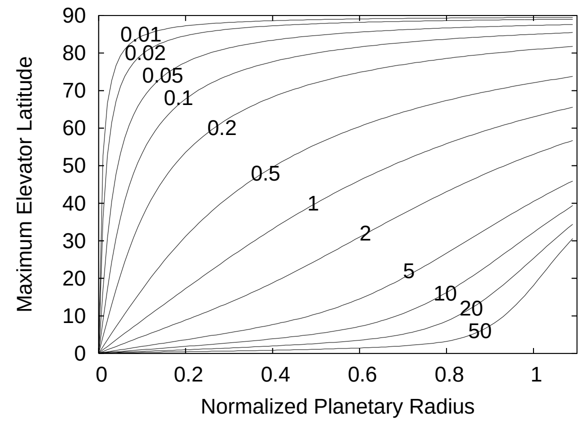

(a) Maximum inclination of 90°.

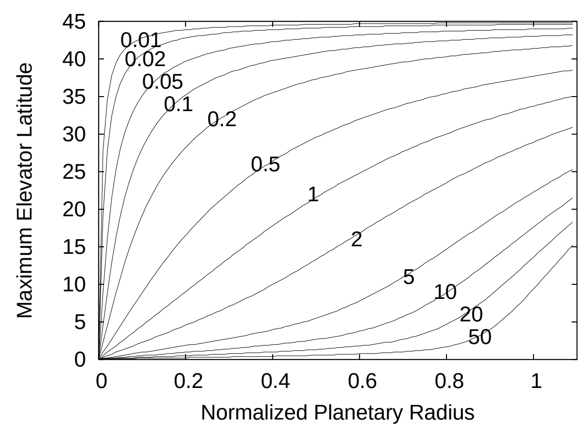

(b) Maximum inclination of 45°.

Figure 5: Maximum reachable latitude as a function of normalized planetary radius for different values of the shape parameter α, assuming maximum tether inclinations at the anchor of 90° and 45°.

the point at which the tether is parallel to the equatorial plane moves out towards infinity, and ceases to exist. At that point, it becomes possible to satisfy the boundary condition at infinity. As the inclination is increased more, the altitude of the counterweight gets lower and lower, as in case (II). Once the altitude of the counterweight reaches the synchronous altitude, satisfying the boundary condition becomes impossible once again. The tether crosses the equatorial plane before reaching the synchronous altitude preventing it from being terminated as in case (III).

We conclude that for a given anchor location, there will generally be a range of inclinations for which a tether shape that satisfies the counterweight boundary condition exists. Within that range, the counterweight altitude decreases from infinity to the synchronous altitude as in Figure 3.

Figure 4 shows the inclinations that lead to valid tether solutions in the case of the Earth space elevator. The graph has been truncated at an inclination of 90°. Higher inclinations are mathematically possible, but the tether would have to go underground for the first part of its length.

3 Maximum Anchor Latitude

As we saw in Figure 4, there is a maximum latitude beyond which no inclination allows the tether to satisfy the counterweight boundary conditions. With Figure 5(a), it is possible to determine the maximum anchor latitude in the general case. This figure was generated by considering, for a given planetary radius and shape parameter, which latitude would lead to an infinitely long tether with 90° inclination.

This figure isn't very useful for practical purposes because it accepts tethers that are very inclined at the base. As we shall see in Section 4.1, such tethers have a small payload. Therefore, we have also considered the case where tether inclination is limited to 45° in Figure 5(b).

Clearly these two figures are very similar except for a different scaling of the vertical axis. By considering a number of limit cases we shall try to explain this similarity and better understand the characteristics of the plots. For clarity we introduce the function $\theta_{max}(\tilde{r}_0, \psi_{max}, \alpha)$ which gives the maximum latitude from the normalized planetary radius, the maximum acceptable tether inclination and the shape parameter.

θ_{max} is the latitude at which a tether inclined by θ_{max} at the anchor is right at the limit between case (I) and case (II). At that limit, the tether solution is infinitely long. So, to study θ_{max}, we shall be studying tether solutions that go to infinity.

3.1 Small Planet Limit

First we shall direct our attention to the case where $\tilde{r}_0 \ll 1$. This approximation corresponds to the case where the planet is small compared to the synchronous altitude (we could also say that the planet rotates slowly compared with an object that would orbit near ground level). This is a good approximation for most known planetary bodies; the gas giants are the main exception. For Earth $\tilde{r}_0 \approx 0.151$ and for Mars $\tilde{r}_0 \approx 0.166$.

As always (see Section 2.3), the angle ϕ decreases with altitude, as does the distance to the equatorial plane. Because the planet is small, the distance to the equatorial plane at the anchor is much smaller than the distance to the synchronous altitude. Therefore, to avoid crossing the equatorial plane, the tether is nearly parallel to the equatorial plane far before the synchronous altitude. This means that any significant tether curvature occurs well below that altitude. Well below synchronous altitude, the centrifugal force term in $\vec{\tilde{g}}(\vec{\tilde{r}})$ can be ignored, so (13) reduces to

$$\frac{\mathrm{d}^2\vec{\tilde{r}}}{\mathrm{d}\tilde{s}^2} = \alpha\left(\frac{\vec{\tilde{r}}}{\tilde{r}^3}\right)_\perp \tag{16}$$

This equation can be normalized by changing the length scale by a factor α

$$\frac{\mathrm{d}^2\vec{\check{r}}}{\mathrm{d}\check{s}^2} = \left(\frac{\vec{\check{r}}}{\check{r}^3}\right)_\perp \tag{17}$$

where the distance $\check{d}$ is the normalized version of $\tilde{d}$ and corresponds to $\tilde{d}/\alpha$. This new normalization is very satisfying as the tether equation contains no constants at all. However, to prevent confusion with the previous normalization of distances, we will avoid this notation whenever possible.

The consequence is that θ_{max} is only a function of $\tilde{r}_0/\alpha$ and ψ_{max}). There is one fewer parameters to consider. In Figure 5, for small values of the normalized planetary radius, the curves for different shape can be deduced from one another by stretching in the horizontal direction.

3.2 Low Curvature Limit

Remaining in the small planet limit, we now consider the case where $\tilde{r}_0/\alpha \gg 1$. In this case, the tether undergoes very little curvature at all. This is particularly clear from (17) where there is very little effect on the tether when $\check{r}$ is large.

If we ignore curvature altogether, we find that the tether is straight. In this approximation, $\theta_{max} \approx \psi_{max}$.

3.3 High Curvature Limit

Still in the small planet limit, we now consider the opposite case in which $\tilde{r}_0/\alpha \ll 1$. In this case, the tether curves sharply if its inclination ψ is not small. If the tether is inclined at its base, it very quickly becomes vertical. This prevents large starting latitudes.

Since the latitude is small and the curvature occurs near the base of the tether, we will make the approximation of a uniform gravity field over a flat planet. In this approximation $\phi \approx -\psi$. We normalize equation (9) and apply the small planet limit to get

$$\frac{\mathrm{d}\phi}{\mathrm{d}\tilde{s}} = -\frac{\alpha}{\tilde{r}_0^2}\sin(\phi) \tag{18}$$

which can be further simplified by taking the derivative with respect to $\tilde{y}$ instead of $\tilde{s}$

$$\frac{\mathrm{d}\phi}{\mathrm{d}\tilde{y}} = -\frac{\alpha}{\tilde{r}_0^2} \tag{19}$$

We now integrate from 0 to y_0, and note that $\phi = 0$ at $y = 0$, to get an expression for the inclination at the anchor

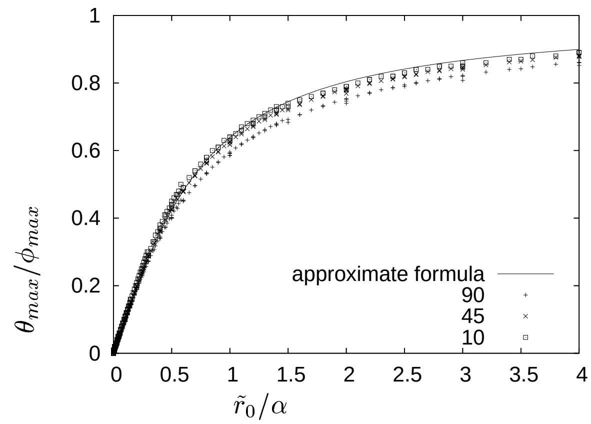

Figure 6: Comparison of (23) with simulation data for maximum inclinations of 10°, 45° and 90°. Only data points with $\tilde{r}_0 < 0.3$ were plotted.

$$\psi_0 = -\phi_0 = \frac{\alpha}{\tilde{r}_0^2} y_0 \tag{20}$$

Finally, we can express y_0 in terms of r_0 and the starting latitude θ_0 as $y_0 \approx r_0 \theta_0$ to get

$$\psi_0 = \frac{\alpha}{\tilde{r}_0} \theta_0 \tag{21}$$

So in the high curvature limit

$$\theta_{max} \approx \frac{\tilde{r}_0}{\alpha} \psi_{max} \tag{22}$$

3.4 A Combined Formula

If $\tilde{r}_0/\alpha$ is near 1 then the analysis becomes much more difficult as both the x and y gravity components are significant. A simple empirical interpolation can nevertheless be used with very good results

$$\theta_{max} \approx \frac{2}{\pi} \psi_{max} \arctan\left(\frac{\pi}{2} \frac{\tilde{r}_0}{\alpha}\right) \tag{23}$$

It is easy to verify that this formula holds in both limit cases. When $\tilde{r}_0/\alpha$ is near 1, this formula gives a result that is up to 8% too high.

Figure 6 illustrates the quality of the approximation. The match is slightly better for low values of the tether inclination. For high inclinations the approximation is slightly optimistic. In this figure we have limited ourselves to $\tilde{r}_0 < 0.3$, for $\tilde{r}_0 > 0.5$ we start to see significant deviation from (23). With larger $\tilde{r}_0$ higher latitudes than expected can be reached.

4 Practical Considerations

So far we have considered whether it was possible to have a space elevator at a given latitude by considering the static tether equation. In practice other considerations will further limit the latitude that can be reached.

4.1 Payload to Elevator Mass Ratio

One of the major concerns in space elevator construction is the ratio of payload mass to elevator mass. Indeed, this ratio determines how much material has to be lifted during the elevator construction for a given elevator capacity.

We saw in Section 1.1 that the taper ratio of a uniform-stress tether only depends on the change in potential along the tether. The potential is uniform at the surface of a planet, and from Figure 2 the potential changes very slowly near the synchronous orbit. Therefore, the taper ratio for non-equatorial space elevators is almost the same as the taper ratio for equatorial space elevators.

In the small planet limit, the angle between the tether and the equatorial plane is small, except possibly near the surface of the planet. Therefore, the length of the tether doesn't depend much on the latitude of the anchor. Moreover, since the potential depends slowly on y, the taper profile of the non equatorial space elevator is nearly the same as the profile for an equatorial one.

Therefore, the only significant difference between equatorial and non-equatorial elevators is due to the tension at the base of the tether not being vertical in the non-equatorial case. Since only the vertical component of the tension can be used to lift a payload, and elevators of equal mass have nearly equal tension at their base, we get a reduced payload to elevator mass ratio in the non-equatorial case:

$$(P/M)_{off-equator} \approx (P/M)_{equator} \cos(\psi_0) \tag{24}$$

Thus to maintain payload when leaving the equator means one has to multiply the elevator mass by $1/\cos(\psi_0)$. For small inclinations at the anchor this inefficiency is insignificant. But approaching inclinations of 90° is clearly out of the question.

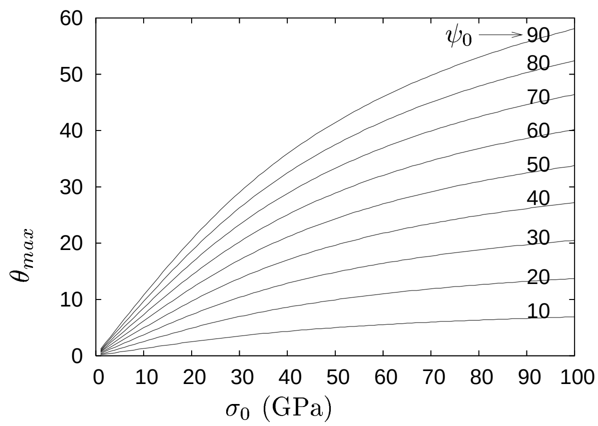

Figure 7: Maximum reachable latitude for an Earth space elevator as a function of σ_0, for different values of the inclination ψ_0.

The designer of Earth space elevators will find Figure 7 useful to quickly determine the maximum elevator latitude as a function of maximum inclination at the anchor. For ease of use σ_0 has been used instead of the shape parameter, the tether density is assumed to be fixed at 1300 $\mathrm{kg/m^3}$.

4.2 Horizontal Force on Anchor

In addition to reducing the payload to mass ratio of the elevator, the inclination at the tether's base causes a horizontal force to be applied to the anchor platform. This force is simply given by:

$$F = T_0 \tan(\psi_0) \tag{25}$$

If the anchor is a mobile ocean platform, this force will need to be countered or else the anchor will drift towards the equator. For heavy lift elevators significantly off the equator, this force will have to be taken into account when selecting the anchor platform.

4.3 Stability

An equatorial tether with very high elasticity (low Young's modulus), or with a small extension beyond the synchronous altitude can be unstable [7]. For equatorial space elevators, we would be considering conditions far from this instability region, so it is of no concern. In the case of non-equatorial elevators, the curvature at the base of the elevator should cause a reduction in the axial stiffness of the tether as seen from the counterweight. We can therefore conjecture that the frequency of the elevator modes will decrease for a non-equatorial elevator. This could cause the instability to occur for realistic tether parameters.

We conjecture that as in the equatorial case, the instability will occur for short tethers, near the boundary between (II) and (III), where the counterweight is just beyond the synchronous altitude (see Section 2.3). However the instability will extend to greater counterweight altitudes. The maximum reachable is determined at the (I)-(II) boundary and should not be affected. However, external effects such as the presence of Earth's Moon may limit the length of the elevator, and thus limit the latitude.

4.4 Deployment

During the initial deployment phase, there is no contact between the tether and the Earth, which takes away the only force keeping the elevator away from the equatorial plane. This leaves two possibilities for deploying a non-equatorial space-elevator.

- A propulsion system can be attached to the bottom of the tether during deployment to keep the tether away from the equatorial plane. For a 10° latitude, and a one ton elevator this option would require hundreds of newtons of thrust over a period of days and is therefore impractical.

- The tether can be deployed in the equatorial plane, attached to the anchor platform, and then moved to its final location away from the equator. If an off-equator location has been selected to avoid interfering with geosynchronous satellites, the initial deployment can be done at a longitude where there is an available geosynchronous slot, after which the elevator can be moved to its final latitude.

4.5 Tether Shape Determined Numerically

Three of the applications we mentioned for non-equatorial space elevators were the avoidance of particular areas in the equatorial plane. In this paper we have not pushed the analysis of (13) far enough to determine whether these obstacles are indeed avoided.

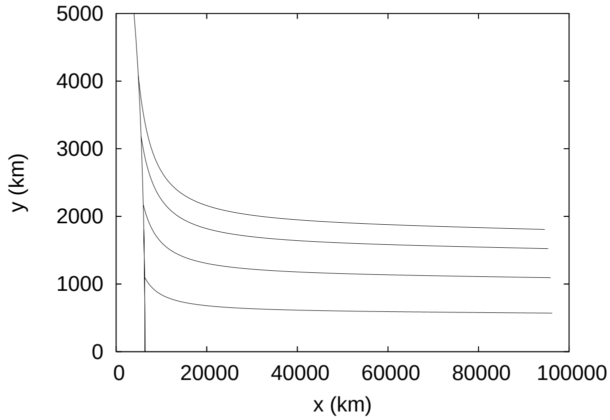

Figure 8: Numerical solutions of the shape equation for the Earth with the standard tether parameters. The length of the tether was set to 90,000 km. Starting latitudes of 10°, 20°, 30° and 40°. Note that the scale is different along the x and y axes.

Figure 8 shows some numerical solutions. They suggest that avoiding the geosynchronous satellites is easy. On the other hand, the most intense areas of the radiation belts extend over 2,000 km above the equatorial plane, which only highly inclined elevators can avoid.

Conclusion

In this paper we have presented the equations that govern the statics of non-equatorial uniform-stress space elevators. These equations have been reduced to a non-dimensional form allowing the analysis to be applied to any tether and planetary parameters.

The tether's taper profile has turned out to be easy to compute as in the equatorial case, once its the spatial configuration is known. Unfortunately, the spatial configuration is difficult to obtain analytically.

Of particular interest to the elevator designer is the maximum anchor latitude for a non-equatorial elevator. This problem has been solved in a few limit cases, and an approximate formula has been proposed.

Off the equator, the tether is not vertical at the base of the elevator. This causes a reduction in payload, which is the major engineering cost of being off the equator. It also causes a horizontal force to be applied to the anchor station, which much be taken into account for an ocean platform.

This study has ignored dynamic effects, in particular the stability of off-equatorial elevators has to be checked. For small latitudes the stability of equatorial elevators carries over, but we expect instabilities to occur in a wider range of conditions than in the equatorial case. This remains to be verified. The effect of climbers on the tether also needs to be studied.

Acknowledgements

I would like to thank Valérie Leblanc for the time she spent proof reading and pointing out bugs.

References

[1] B. Edwards and E. Westling, *The Space Elevator*. Spageo Inc., 2002.

[2] Y. Artsutanov, "V kosmos na electrovoze (into space with the help of an electric locomotive)," *Komsomolskaya Pravda*, 1960.

[3] V. Lvov, "Sky-hook: Old idea," *Nature*, vol. 158, no. 3803, pp. 946–947, Nov. 1967.

[4] J. Pearson, "The orbital tower: a spacecraft launcher using the Earth's rotational energy." *Acta Astronautica*, vol. 2, pp. 785–799, 1975.

[5] A. C. Clarke, *The Fountains of Paradise*. Warner Books, 1978.

[6] A. M. Jorgensen, R. G. Morgan, B. Gassend, R. H. W. Friedel, and T. Cayton, "Space elevator radiation hazards and how to mitigate them," in *Proceedings of the* $3^r d$ *Annual International Space Elevator Conference*, June 2004.

[7] V. V. Beletsky and E. M. Levin, *Dynamics of Space Tether Systems*, ser. Advances in the Astronautical Sciences. Amer Astronautical Society, August 1993, vol. 83.